New Family of Ionic Supersalts with Covalent-like Directionality and Unconventional Multiferroicity

Yaxin Gao
Huazhong University of Science and Technology
Menghao Wu (wmh198789@163.com)
Huazhong University of Science and Technology https://orcid.org/0000-0002-1683-6449
Puru Jena
Virginia Commonwealth University

Article

Keywords: Ionic crystals, supersalts, PnH4FeX4, ionic bonding

Posted Date: August 18th, 2020

DOI: https://doi.org/10.21203/rs.3.rs-53130/v1

Version of Record: A version of this preprint was published at Nature Communications on February 26th, 2021. See the published version at https://doi.org/10.1038/s41467-021-21597-3.

Abstract

Ionic crystals composed of elemental ions such as NaCl are centro-symmetric and, thus, non-polar due to directionless ionic bonding interactions. To develop polar materials, the directionality feature of covalent bonding is necessary. Here, we propose a novel way where ionically bonded crystals can develop polarity by changing their building blocks from elemental ions to cluster-ions. Superalkalis and superhalogens are clusters which mimic the chemistry of alkali and halogen atoms. Equally important, unlike the elemental ions, the geometries of these superions are not spherical. Endowed with these unique features, ionic supersalts form anisotropic polar structures with ionic bonding, yet covalent-like directionality, akin to sp^3 hybridized systems. Using density functional theory and extensive structure searches, we predict a series of stable supersalts, PnH_4MX_4 (Pn = N, P; M = B, Al, Fe; X = Cl, Br) composed of superalkali PnH_4 and superhalogen MX_4 ions with unprecedented properties: (1) ferroelectricity with ultra-long ion displacements (~ 3 Å); (2) ferroelasticity with ultra-large reversible strain (> 40%); and (3) both with ultra-low switching barriers (about 6 to 13 meV/atom). These values are inconceivable in traditional ferroelectric/ferroelastic materials owing to their brittle covalent nature. Coupling of ferroelectricity with ferroelasticity can further enable strain-controlled polarization as well as electrically-controlled strain. In particular, PnH_4FeX_4 exhibits triferroic coupling of ferroelectricity, ferroelasticity, and antiferromagnetism where the spin directions can be altered via either ferroelastic or 90-degree ferroelectric switching. These ionic supersalts can be synthesized using facile solution-processed fabrication by exothermic reactions, $MPn + 4HX \rightarrow PnH_4MX_4$ or $PnH_4X + MX_3 \rightarrow PnH_4MX_4$, which may open a new chapter in multiferroics.

Introduction

Ionic crystals composed of elemental ions are non-polar due to the directionless feature of ionic bondings. In this paper we propose a paradigm shift in material synthesis where ionic crystals can be designed to exhibit directional bonding and lead to unprecedented materials with long ion-displacement ferroelectricity, high-strain ferroelasticity, and triferroic couplings. The key is to change the building blocks ionic crystals from elemental ions to cluster ions. This concept was introduced by Khanna and Jena more than 25 years ago when the authors showed that superatomic [1, 2, 3] clusters with appropriate size and composition can be designed to mimic the properties of atoms and when assembled could form materials with unique properties. Superhalogens and superalkalis proposed by Gutsev and Boldyrev [4, 5, 6, 7] much earlier belong to a sub-group of superatoms. Superhalogens have electron affinities (EAs) that are larger than those of halogens (~ 3.6 eV for Cl) while superalkalis [8, 9, 10, 11] have ionization potentials (IPs) that are smaller than those of alkalis (~ 3.9 eV for Cs). Prominent examples include superhalogens with formula unit AX_{k+1} where k the valence of atom A and X is a halogen atom (e.g., BX_4, AlX_4, SiX_5 and PX_6), and superalkalis with formula unit $M_{k+1}L$, where M is an alkali atom and k is the formal valence of the electronegative atom L (e.g., Li_3O, Li_4N). The former can be used for oxidation of counterpart systems with high IPs and production of organic superconductors, [12] while the latter can find applications in the synthesis of charge-transfer salts where the anions are formed by the species with low EAs. Giri et. al. [13] have shown that superalkalis and superhalogens can be combined together to form a new class of supersalts where both the ions retain their structural and compositional identity. Supersalts with tailored properties [13, 14], superbases with strong basicity [15], and alkalides with negatively charged alkali metals have been discussed in the literature. [13, 16] Similarly, superalkali and superhalogen species have been used to construct perovskites for photovoltaics [17, 18], lithium superionic conductors [19], etc.. Experimentally, a series of

superatomic solids assembled from molecules, like nickel telluride clusters and fullerenes, [20] have been successfully synthesized, [21] and interesting properties like controllable phase transitions have been studied.[22, 23, 24, 25] However, the reports on supersalts composed of both superalkali and superhalogen ions are still scarce. For example, in the supersalt Na_3OBH_4 the superalkali Na_3O has tetrahedral geometry while it is planar when held in isolation.[26]

The bonding between adjacent superalkali cations and superhalogen anions in supersalts is ionic. Generally, ionic solids adopt structures with higher coordination numbers to maximize the ionic bonding, increase the Madelung constant, and, hence, reduce the lattice energy. As a result, typical structures of ionic binary systems like alkali halides are non-polar rock salt (RS) or Cesium Chloride (CsCl) types where the coordination numbers are, respectively, 6 and 8. They all are non-polar centro-symmetrical structures due to directionless ionic bonding interactions. In contrast, the directionality and saturation of covalent bonding could favor the formation of crystalline polarization. According to the Philips scale, when the ionicity declines below the critical value 0.785, marking the idealized boundary between predominantly “covalent” and “ionic” systems [27], zinc-blende (ZB) structure with lower coordination will become energetically more favorable, e.g., BN (0.256), AlP (0.307), ZnS (0.623), etc. Those structures are polar, although their polarizations are not switchable due to the brittle nature of covalent bonding. Mixed ionic-covalent bonding may facilitate the formation of switchable polarization with moderate barriers (i.e., ferroelectricity), which has been revealed in well-known perovskite ferroelectrics [28] ($BaTiO_3$, $PbTiO_3$, etc.). However, we note that supersalts may not necessarily adopt the non-polar structures for most ionic systems: compared with isotropic single atoms, the anisotropic geometry of superatoms may give rise to breaking of centro-symmetry. If such breaking can induce switchable polarization, highly ionic ferroelectrics might be formed via facile and solution-processed [29] fabrications, offering a route for large-scale production that cannot be applied to conventional ferroelectrics. This, in turn, can find promising applications in a broad range of fields including nonvolatile memories, sensor and actuators, nonlinear optical materials, etc.

In this paper, using *ab initio* methods, we design a series of stable supersalts PnH_4MX_4 (Pn = N, P; M = B, Al, Fe; X = Cl, Br) composed of superalkali, PnH_4 and superhalogen, MX_4, which may enable facile fabrication by exothermal reactions $MPn + 4HX \rightarrow PnH_4MX_4$ or $PnH_4X + MX_3 \rightarrow PnH_4MX_4$. These ionic systems are likely to form intriguing distorted ZB structure, instead of non-polar centro-symmetrical structure. The covalent-like directionality gives rise to unprecedented ferroelectricity with long ion-displacement (~ 3 Å) and ferroelasticity with large reversible strain (> 40%), which are multiferroically coupled. [30] Conventional ferroelectrics and ferroelastics, owing to the brittle nature of covalent bonding, cannot sustain such large deformations as the high energy barriers may induce fracture. In these ionic supersalts, however, the long-range Coulomb interaction between cations and anions may greatly reduce such barriers to ultra-low magnitude of only ~ 0.1 eV/f.u. or ~ 10 meV/atom. It is noteworthy that the experimental realization of multiferroics with two coupling ferroics (biferroics) is still challenging due to the mutual exclusive origins of different ferroics. [31] Herein, PnH_4FeX_4 is revealed to be even an intrinsic triferroics with coupled ferroelectricity, ferroelasticity, and antiferromagnetism, where the spin directions can be altered via either ferroelastic switching or 90-degree ferroelectric switching. This, in turn, can render desirable giant anisotropic magnetoresistance for non-volatile memories that can be controlled by either electric field or strain.

Table 1
The polarization of PnH_4MX_4 and the energy change for the reaction $PnH_4X + MX_3 \rightarrow PnH_4MX_4$, where negative values indicate exothermal.

	NH_4BCl_4	NH_4BBr_4	PH_4BCl_4	PH_4AlCl_4	PH_4FeCl_4	PH_4BBr_4	PH_4AlBr_4	PH_4FeBr_4
ΔE (eV/f.u.)	-0.14	-0.05	-0.23	-0.55	-0.63	-0.12	-0.48	-0.89
P($\mu C/cm^2$)	13.8	12.4	13.1	11.7	11.7	11.8	10.6	10.7

Results And Discussion

The model of ZB, RS and CsCl structures are displayed in Fig. 1(a), where the ZB lattice can either adopt an 8-atom cubic cell (left) or a smaller 4-atom unit cell (right). First, we select superalkali NH_4 and superhalogen BCl_4 for constructing a supersalt NH_4BCl_4, where both superatoms are non-centrosymmetric compared with isotropic single atoms, as shown in Fig. 1(b). After an extensive structure search using the CALYPSO code, we obtain the ground state structure of supersalt NH_4BCl_4 displayed in Fig. 1(c), which is non-centrosymmetric with independent superalkali NH_4 and superhalogen BCl_4 ions. It is a distorted zinc-blende (dZB) structure where the lattice constants (|a|:|b|:|c|=$\sqrt{2}$:$\sqrt{2}$:1) are relatively doubled in |a| and |b| (or contracted by half in |c|) compared with the 4-atom unit cell of standard ZB (|a|:|b|:|c|=1:1:$\sqrt{2}$). This structure is 0.08 and 0.44 eV/f.u. lower in energy compared with corresponding RS and CsCl structures, respectively. Similar to ZB phase, each superalkali cation in the dZB supersalt is tetrahedrally bonded with four adjacent superhalogen anions and vice versa, akin to sp^3 hybridization of covalent bonding, which are also connected by weak H…Cl hydrogen bonds (with bond length ~ 2.4 Å). The energy release computed for a hypothetical reaction $BN + 4HCl \rightarrow NH_4BCl_4$, is as high as 1.10 eV/f.u. (i.e., ΔE=-1.10 eV/f.u.), which may enable its solution-processed synthesis via etching of boron nitride by acid. We also examined the following reactions:

$NH_4BCl_4 \rightarrow NH_4Cl + BCl_3$, ΔE = 0.14 eV/f.u.,

$NH_4BCl_4 \rightarrow NH_3BCl_3 + HCl$, ΔE = 0.41 eV/f.u.,

These hypothetical decompositions are all endothermal, which confirms the chemical stability of NH_4BCl_4 and impedes the formation of other products like NH_4Cl or NH_3BCl_3 during the synthesis. However, the strong covalent B-N bonding of BN may lead to high energy cost to break those bonds, so we cannot guarantee the formation $BN + 4HCl \rightarrow NH_4BCl_4$ would spontaneously proceed at ambient conditions. On the other hand, the reaction $NH_4Cl + BCl_3 \rightarrow NH_4BCl_4$ might be a more feasible route for the fabrication of NH_4BCl_4. For the same group pnictides like BP, AlN, the bondings are weaker and the larger hollow space may enable protons or halogen anions to permeate from the surface to inside, which should facilitate similar formations of supersalts. Hence, we further searched a series of low-energy structures for NH_4MX_4/PH_4MX_4 supersalts. As shown in Fig. 1(c), the ground state of NH_4BBr_4 shares the same type of dZB structure with NH_4BCl_4, which is similar to the case for PH_4BCl_4, PH_4AlCl_4, PH_4BBr_4, PH_4BBr_4, with a slight difference in the relative angles between the cation tetrahedrons and anion tetrahedrons. 3d metal like Fe may also be used to construct superhalogen like $FeCl_4$, and the corresponding supersalts like PH_4FeCl_4, PH_4FeBr_4 turn out to possess similar dZB ground state

structures. Their formations are all energetically favorable, with positive energy releases as listed in Table 1. There are a few exceptions like NH_4BF_4 and NH_4AlCl_4 that prefer to form structures where each superalkali cation is hydrogen-bonded to 8 adjacent superhalogen anions and vice versa, while NH_4AlF_4 forms a layered perovskite structure, as shown in the right panel of Fig. 1(c).

Next, we focus on the polar dZB structures in Fig. 1(c), which could be ferroelectric as long as their polarizations are switchable. In previous studies, [32, 33] the computed switching barriers for ZB structures like CuCl and ZnO can be over 0.30 eV/f.u., so their polarizations are difficult to reverse under ambient conditions. Compared to the breaking of covalent bonds in those structures during polarization switching, the energy barrier for ion displacement in ionic supersalts should be much lower. Taking NH_4BCl_4 shown in Fig. 2(a) as the paradigmatic case, if all the NH_4 cations at the initial ground state (I) are simultaneously displaced by 2.63 Å along –y direction, with the rotation of all superatoms by a certain angle along –y axis, an equivalent structure (III) with a reversed polarization can be obtained. The reversed polarization turns out to be of a considerable value, namely, 13.8 μC/cm^2 as listed in Table 1. Its band structure in Fig. 2(b) reveals that the system is insulating with a large bandgap over 5 eV, which should result in high dielectric breakdown voltage. The ferroelectric switching pathway is computed by SSNEB calculations in Fig. 2(c), with a symmetric state as the intermediate state (II), revealing a switchable barrier of only 0.13 eV/f.u. (0.013 eV/atom). Such a high ion displacement with such a small switching barrier is unimaginable in traditional ferroelectrics. For example, the ion displacement in $PbTiO_3$ during ferroelectric switching is far below 1 Å, while the barrier is even larger (~ 0.15 eV/f.u., i.e., 0.03 eV/atom).[34]

The dynamical stability of the polar ground state for NH_4BCl_4 is further verified by the phonon spectra in Fig. S1, which shows no imaginary frequencies in all vibration spectra. For the nonpolar intermediate state II (paraelectric phase), the imaginary soft optical modes will lead to both rotation and translational displacement of NH_4 cations and BCl_4 anions away from the centrosymmetric position, giving rise to the spontaneous symmetry-breaking below the Curie temperature. Born-Oppenheimer molecular dynamics (BOMD) simulations are also performed to check its thermal stability. Snapshots of the equilibrium structure for NH_4BCl_4 at 300 K and at the end of 5 ps are shown in Fig. S2, suggesting the robustness of its ferroelectricity at ambient conditions. Similar mechanism of ferroelectric switching can be applied to other supersalts like PH_4BBr_4 via the displacement of cations and anions (2.86 Å along –y direction). The switching barrier in this case is also around 0.13 eV/f.u. (i.e., 0.013 eV/atom, as shown in Fig. 3(c)). The only difference is the rotational mode of superatoms during ferroelectric switching, as displayed in Fig. S3.

We note that the dZB structure is relatively elongated in two directions, i.e., contracted in the third direction compared with standard ZB phase, which is actually a spontaneous strain that might be switched via stress. The pathway for such ferroelastic switching for NH_4BCl_4 is calculated by SSNEB method, where a symmetrical non-polar state P(0) can be the intermediate state as its polarization switched from –z direction at the initial P(-z) state to –x/–y direction at the final state P(-x)/P(-y), as shown in Fig. 3(a) and (b). Here, the superiority of ionic ferroelastics with long-range Coulomb interactions between ions can be highlighted, as a barrier of only 0.065 eV/f.u. (i.e., 0.0065 eV/atom) is required for reversing such a high ferroelastic strain (defined as (|b|/|c|-1) × 100%) more than 40%. For high-strain (> 20%) ferroelastics predicted in previous reports, [35, 36, 37, 38] the switching barriers (up to 0.5 eV/atom) are almost orders of magnitude higher, which can be attributed to the distinct features of covalent bonds in those systems. Moreover, the ferroelectric polarization is also rotated by 90

degree upon ferroelastic switching. Such 90-degree polarization switching can also be achieved if an external electric field is applied along −x or −y direction. Hence, the ferroelectricity and ferroelasticity are coupled, so we can use strain to control the polarization direction and electric field to control strain. Due to the low barrier, the required electric field or stress for reversing such a large strain can be greatly reduced.

Supersalts with 3d magnetic ions like PH_4FeBr_4 also possess similar coupled ferroelectricity and ferroelasticity. Moreover, their magnetism can also be coupled. We have checked different possible spin configurations (see Table S1) for PH_4FeBr_4.Tthe ground state is displayed in Fig. 4(a), which is antiferromagnetic where the spins of two Fe ions in the unitcell are of opposite direction, while the spins on the same lines along −x, −y or −z direction are of the same direction. Further, spin non-collinear calculations reveal a magnetic anisotropy energy of 0.4 meV for the spin of each Fe atom, where the spins prefer to be aligned along −y direction, the “contracted” direction in Fig. 4(a). However, as the “contracted” direction is switched to −x direction upon ferroelastic switching, i.e., 90-degree ferroelectric switching, the magnetization easy axis is also switched from −y to −x direction. Equivalently, it might also be switched to −z direction via a strain or electric field along −z direction. Compared with NH_4BCl_4, the switching barrier of PH_4FeBr_4, according to the calculated pathway in Fig. 4(b), is larger (~ 0.13 eV/f.u.), while the bandgap is much more reduced (~ 1 eV, see Fig. 4(c)) to a desirable range for nanoelectronics. Hence, magnetism is also coupled with ferroelectricity and ferroelasticity in PH_4FeBr_4, which can be viewed as a multiferroic material with “triferroic” coupling. Such coupling may render electrically-controlled giant anisotropic magnetoresistance for non-volatile memories, which is highly desirable but still challenging in the current developing field of antiferromagnetic spintroincs.[39]

Conclusions

In summary, using an unbiased structure search based on DFT calculations, we predict a series of stable ionic supersalts PnH_4MX_4 composed of superalkali PnH_4 and superhalogen MX_4 ions. The reactions $MPn + 4HX \rightarrow PnH_4MX_4$ or $PnH_4X + MX_3 \rightarrow PnH_4MX_4$, which are all exothermic, may render facile and large-scale fabrication of these super ionic salts. These supersalts form intriguing distorted ZB structures that favor covalent systems with directional bonding. This unique property is attributed to the anisotropy induced by superatoms. The special configuration enables ferroelectricity with ultra-long ion displacement, as well as ferroelasticity with ultra-large reversible strain. Coupled together, one can realize strain-controllable polarization as well as electrically-controllable strain. The ionic bonding features reduce the switching barriers with such large deformations to only around ~ 0.1 eV/f.u.(~ 10 meV/atom), which is inconceivable in conventional ferroelectrics and ferroelastics because it cannot be sustained due to the brittle nature of covalent bonding. Finally, we show that PnH_4FeX_4 is triferroics with coupled ferroelectricity, ferroelastcity, and antiferromagnetism, where the spin distribution can be altered via either ferroelastic switching or 90- degree ferroelectric switching. Since supersalts and triferroics are both long-sought but still unrealized to date, our findings may offer new ideas and stimulate experimental efforts in those fields.

Methods

Computational Methods

Our theoretical calculations are based on density-functional-theory (DFT) methods implemented in the Vienna Ab initio Simulation Package (VASP 5.3) code.[40, 41] The Perdew-Burke-Ernzerhof (PBE) [42] functional within the generalized gradient approximation for the exchange and correlation potential, together with the projector-augmented wave (PAW) [43] method, are adopted. The kinetic energy cut-off is set to 520 eV in all calculations. The Brillouin zones are sampled by Monkhorst–Pack scheme [44], which is set to 5 × 7 × 5 for the unit cell. The shape and volume of each unit cell are fully optimized, and the convergence threshold for self-consistent-field iteration is set to be 10^{-6} eV. Computed forces at all atoms are less than 0.01 eV/Å after the geometry optimization. The van der Waals interactions are taken into consideration by using DFT-D3 functional of Grimme. [45] The Berry phase method [46] is employed to evaluate ferroelectric polarizations, while the ferroelectric/ferroelastic switching pathway is obtained by using a generalized solid-state elastic band (G-SSNEB) method. [47] The phonon calculations are performed using a finite displacement method as implemented in the PHONOPY program. [48] An unbiased swarm-intelligence structural method based on the particle swarm optimization (PSO) technique implemented in the Crystal structure AnaLYsis by Particle Swarm Optimization (CALYPSO) code[49, 50, 51] is employed to search for low-energy structures of supersalts.

Declarations

Competing Interests

The authors declare no competing interest.

Contributions

M. W. designed research; Y.G performed research; Y. G., M. W. and P. J. wrote the paper.

Acknowledgment

We thank all the heroes who have fought against COVID-19. P. J. acknowledges partial support by the U.S. Department of Energy, Office of Basic Energy Sciences, Division of Materials Sciences and Engineering under Award DE-FG02-96ER45579.

References

1. Khanna S, Jena P. Assembling crystals from clusters. *Physical review letters* **69,**1664(1992).
2. Khanna S, Jena P. Atomic clusters: Building blocks for a class of solids. *Physical Review B* **51,**13705(1995).
3. Jena P. Beyond the Periodic Table of Elements: The Role of Superatoms. *J Phys Chem Lett* **4,**1432-1442(2013).
4. Gutsev G, Boldyrev A. DVM-Xα calculations on the ionization potentials of MXk+ 1− complex anions and the electron affinities of MXk+ 1 "superhalogens". *Chemical Physics* **56,**277-283(1981).

5. Gutsev G, Boldyrev A. The theoretical investigation of the electron affinity of chemical compounds. *Advances in chemical physics***,**169-221(1985).

6. Wang X-B, Ding C-F, Wang L-S, Boldyrev AI, Simons J. First experimental photoelectron spectra of superhalogens and their theoretical interpretations. *The Journal of chemical physics* **110,**4763-4771(1999).

7. Elliott BM, Koyle E, Boldyrev AI, Wang X-B, Wang L-S. MX3-superhalogens (M= Be, Mg, Ca; X= Cl, Br): A photoelectron spectroscopic and ab initio theoretical study. *The Journal of Physical Chemistry A* **109,**11560-11567(2005).

8. Rehm E, Boldyrev AI, Schleyer PvR. Ab initio study of superalkalis. First ionization potentials and thermodynamic stability. *Inorganic Chemistry* **31,**4834-4842(1992).

9. Zakrzewski VG, von Niessen W, Boldyrev AI, von Ragué Schleyer P. Green function calculation of ionization energies of hypermetallic molecules. *Chemical physics* **174,**167-176(1993).

10. Gutsev GL, Boldyrev A. DVM Xα calculations on the electronic structure of "superalkali" cations. *Chemical Physics Letters* **92,**262-266(1982).

11. Alexandrova AN, Boldyrev AI. σ-Aromaticity and σ-antiaromaticity in alkali metal and alkaline earth metal small clusters. *The Journal of Physical Chemistry A* **107,**554-560(2003).

12. Wudl F. From organic metals to superconductors: Managing conduction electrons in organic solids. *Accounts of Chemical Research* **17,**227-232(1984).

13. Srivastava AK, Misra N. Novel (Li2X)+(LiX2)− supersalts (X= F, Cl) with aromaticity: a journey towards the design of a new class of salts. *Molecular Physics* **112,**2621-2626(2014).

14. Huang C, Fang H, Whetten R, Jena P. Robustness of Superatoms and Their Potential as Building Blocks of Materials: Al13− vs B(CN)4−. *J Phys Chem C* **124,**6435-6440(2020).

15. Srivastava AK, Misra N. OLi3O− anion: Designing the strongest base to date using OLi3 superalkali. *Chemical Physics Letters* **648,**152-155(2016).

16. Giri S, Behera S, Jena P. Superalkalis and superhalogens as building blocks of supersalts. *The Journal of Physical Chemistry A* **118,**638-645(2014).

17. Fang H, Jena P. Super-ion inspired colorful hybrid perovskite solar cells. *Journal of Materials Chemistry A* **4,**4728-4737(2016).

18. Zhou T, Zhang Y, Wang M, Zang Z, Tang X. Tunable electronic structures and high efficiency obtained by introducing superalkali and superhalogen into AMX3-type perovskites. *Journal of Power Sources* **429,**120-126(2019).

19. Fang H, Jena P. Li-rich antiperovskite superionic conductors based on cluster ions. *Proceedings of the National Academy of Sciences* **114,**11046-11051(2017).

20. Lee C-H, Liu L, Bejger C, Turkiewicz A, Goko T, Arguello CJ*, et al.* Ferromagnetic ordering in superatomic solids. *Journal of the American Chemical Society* **136,**16926-16931(2014).

21. Ong W-L, O'Brien ES, Dougherty PS, Paley DW, Higgs III CF, McGaughey AJ*, et al.* Orientational order controls crystalline and amorphous thermal transport in superatomic crystals. *Nature materials* **16,**83(2017).

22. Pinkard A, Champsaur AM, Roy X. Molecular clusters: Nanoscale building blocks for solid-state materials. *Accounts of chemical research* **51,**919-929(2018).

23. Turkiewicz A, Paley DW, Besara T, Elbaz G, Pinkard A, Siegrist T*, et al.* Assembling hierarchical cluster solids with atomic precision. *Journal of the American Chemical Society* **136,**15873-15876(2014).

24. Zhong X, Lee K, Choi B, Meggiolaro D, Liu F, Nuckolls C*, et al.* Superatomic Two-Dimensional Semiconductor. *Nano letters* **18,**1483-1488(2018).

25. O'Brien ES, Trinh MT, Kann RL, Chen J, Elbaz GA, Masurkar A*, et al.* Single-crystal-to-single-crystal intercalation of a low-bandgap superatomic crystal. *Nature chemistry* **9,**1170(2017).

26. Sun Y, Wang Y, Liang X, Xia Y, Peng L, Jia H*, et al.* Rotational Cluster Anion Enabling Superionic Conductivity in Sodium-Rich Antiperovskite Na3OBH4. *J Am Chem Soc* **141,**5640-5644(2019).

27. Phillips JC. Ionicity of the Chemical Bond in Crystals. *Rev Mod Phys* **42,**317-356(1970).

28. Cohen RE. Origin of ferroelectricity in perovskite oxides. *Nature* **358,**136-138(1992).

29. Li L, Wu MH, Zeng XC. Facile and Versatile Functionalization of Two-Dimensional Carbon Nitrides by Design: Magnetism/Multiferroicity, Valleytronics, and Photovoltaics. *Adv Fun Mater* **29,**1905752(2019).

30. Wu M, Zeng XC. Intrinsic Ferroelasticity and/or Multiferroicity in Two-Dimensional Phosphorene and Phosphorene Analogues. *Nano Lett* **16,**3236-3241(2016).

31. Dong S, Liu J-M, Cheong S-W, Ren Z. Multiferroic materials and magnetoelectric physics: symmetry, entanglement, excitation, and topology. *Advances in Physics* **64,**519-626(2015).

32. Gao Y, Wu M, Zeng XC. Phase transitions and ferroelasticity–multiferroicity in bulk and two-dimensional silver and copper monohalides. *Nanoscale Horizons* **4,**1106-1112(2019).

33. Li L, Wu M. Binary Compound Bilayer and Multilayer with Vertical Polarizations: Two-Dimensional Ferroelectrics, Multiferroics, and Nanogenerators. *ACS nano* **11,**6382-6388(2017).

34. Tadmor EB, Waghmare UV, Smith GS, Kaxiras E. Polarization switching in PbTiO3: an ab initio finite element simulation. *Acta Materialia* **50,**2989-3002(2002).

35. Wu M, Fu H, Zhou L, Yao K, Zeng XC. Nine New Phosphorene Polymorphs with Non-Honeycomb Structures: A Much Extended Family. *Nano Lett* **15,**3557-3562(2015).

36. Li W, Li J. Ferroelasticity and domain physics in two-dimensional transition metal dichalcogenide monolayers. *Nat Commun* **7,**10843(2016).

37. Kou L, Ma Y, Tang C, Sun Z, Du A, Chen C. Auxetic and Ferroelastic Borophane: A Novel 2D Material with Negative Possion's Ratio and Switchable Dirac Transport Channels. *Nano Lett* **16,**7910-7914(2016).

38. Zhang C, Nie Y, Sanvito S, Du A. First-Principles Prediction of a Room-Temperature Ferromagnetic Janus VSSe Monolayer with Piezoelectricity, Ferroelasticity, and Large Valley Polarization. *Nano Lett* **19,**1366-1370(2019).

39. Wadley P, Howells B, Železný J, Andrews C, Hills V, Campion RP*, et al.* Electrical switching of an antiferromagnet. *Science* **351,**587-590(2016).

40. Kresse G, Furthmüller J. Efficient iterative schemes for ab initio total-energy calculations using a plane-wave basis set. *Physical review B* **54,**11169(1996).

41. Kresse G, Furthmüller J. Efficiency of ab-initio total energy calculations for metals and semiconductors using a plane-wave basis set. *Computational materials science* **6,**15-50(1996).

42. Perdew JP, Burke K, Ernzerhof M. Generalized gradient approximation made simple. *Physical review letters* **77,**3865(1996).

43. Blöchl PE. Projector augmented-wave method. *Physical review B* **50,**17953(1994).

44. Monkhorst HJ, Pack JD. Special points for Brillouin-zone integrations. *Physical review B* **13,**5188(1976).

45. Grimme S, Antony J, Ehrlich S, Krieg H. A consistent and accurate ab initio parametrization of density functional dispersion correction (DFT-D) for the 94 elements H-Pu. *The Journal of chemical physics* **132,**154104(2010).

46. King-Smith R, Vanderbilt D. Theory of polarization of crystalline solids. *Physical Review B* **47,**1651(1993).

47. Sheppard D, Xiao P, Chemelewski W, Johnson DD, Henkelman G. A generalized solid-state nudged elastic band method. *The Journal of chemical physics* **136,**074103(2012).

48. Togo A, Tanaka I. First principles phonon calculations in materials science. *Scripta Materialia* **108,**1-5(2015).

49. Wang Y, Lv J, Zhu L, Ma Y. Crystal structure prediction via particle-swarm optimization. *PhysRevB* **82,**094116(2010).

50. Wang Y, Lv J, Zhu L, Ma Y. CALYPSO: A method for crystal structure prediction. *Computer Physics Communications* **183,**2063-2070(2012).

51. Lv J, Wang Y, Zhu L, Ma Y. Particle-swarm structure prediction on clusters. *The Journal of chemical physics* **137,**084104(2012).

Figures

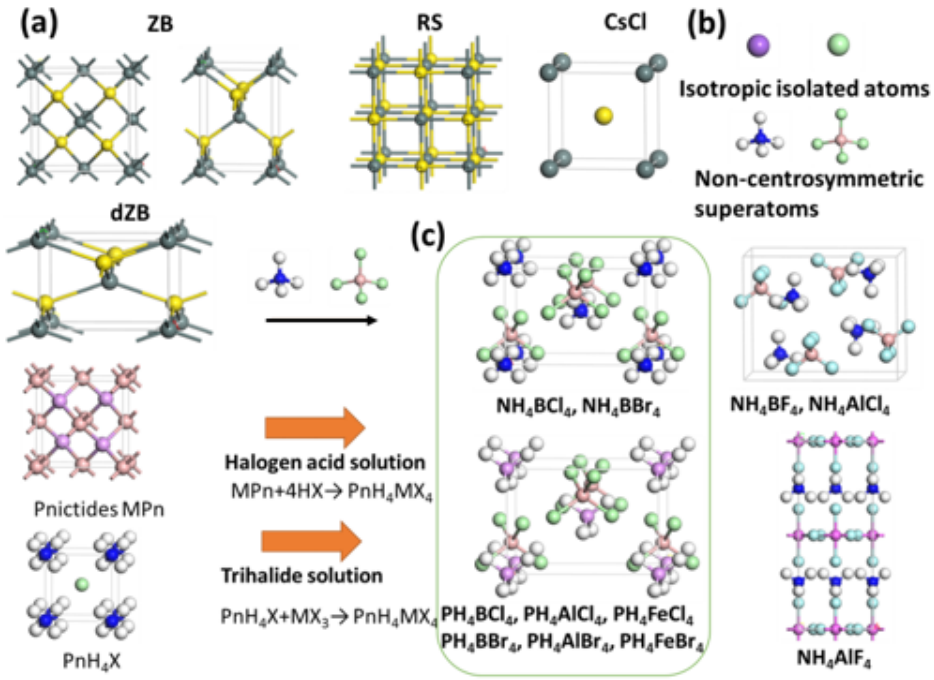

Figure 1

(a) Structures of ZB, dZB, RS and CsCl phase, where dark green and yellow spheres, respectively, denote cations and anions. (b) Non-centro-symmetric superalkali and superhalogen compared with isotropic isolated atoms. (c) Several typical structures of supersalts PnH4MX4, which may be synthesized by reactions MPn+4HX→PnH4MX4 or PnH4X+MX3→PnH4MX4. White, pink, blue, purple and light green spheres denote H, B, N, P and halogen atoms, respectively.

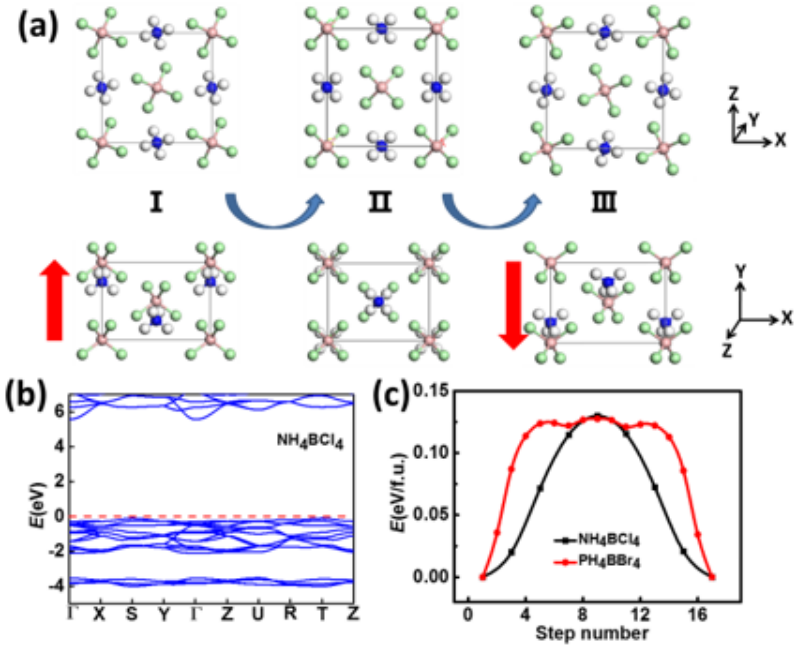

Figure 2

(a) Illustration of ferroelectric switching pathway for NH4BCl4 and (b) its band structure. (c) Comparison of ferroelectric switching pathway between NH4BCl4 and PH4BBr4. The polarization directions are denoted by the red arrows.

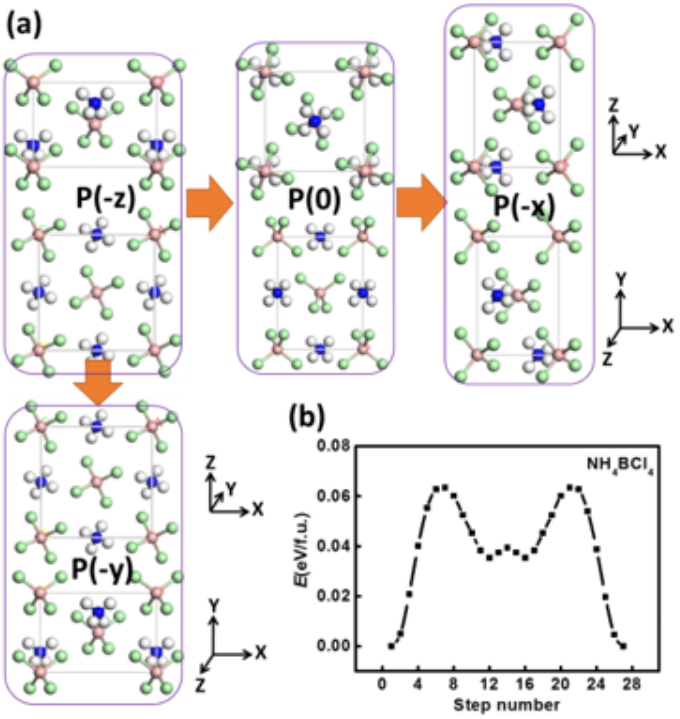

Figure 3

(a) Two equivalent ferroelastic switching for NH4BCl4 with its polarization initially along –z direction switched to either –x or –y direction. (b) Computed ferroelastic switching pathway via SSNEB.

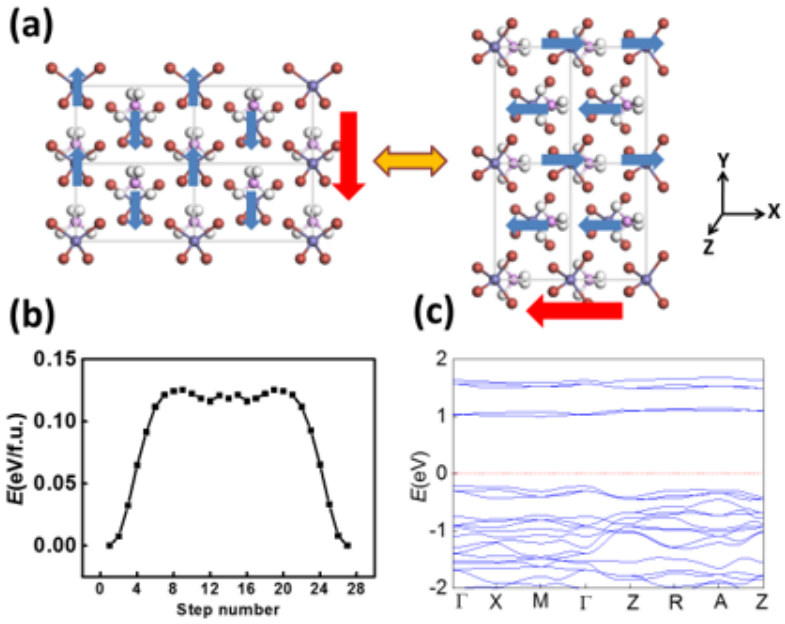

Figure 4

(a) Spin switching upon ferroelastic switching (90-degree ferroelectric switching), (b) ferroelastic switching pathway calculated by SSNEB method, and (c) the band structure for PH4FeBr4. Red and blue arrows denote polarization and spin directions, respectively.

Supplementary Files

This is a list of supplementary files associated with this preprint. Click to download.

- FigS1.png
- FigS2.png
- FigS3.png
- FigS4.png
- TableS1.png